Experiments in Transitional Boundary Layers with Emphasis on High Free-Stream Disturbance Level, Surface Concave Curvature and Strong Favorable Streamwise Pressure Gradient Effects

T. W. Simon and R. J. Volino
University of Minnesota
Mechanical Engineering Department
Minneapolis, MN 55455

Experiments on boundary layer transition with flat, concave and convex walls and various levels of free-stream disturbance and with zero and strong streamwise acceleration have been conducted. Measurements of both fluid mechanics and heat transfer processes were taken. Examples are profiles of mean velocity and temperature; Reynolds normal and shear stresses; turbulent streamwise and cross-stream heat fluxes; turbulent Prandtl number; and streamwise variations of wall skin friction and heat transfer coefficient values. Free-stream turbulence levels were varied over the range from about 0.3% to about 8%. The effects of curvature on the onset of transition under low disturbance conditions are clear; concave curvature leads to an earlier and more rapid transition and the opposite is true for convex curvature. This was previously known but little documentation of the transport processes in the flow was available. When at elevated free-stream disturbance levels, the curvature effect on the onset of transition is greatly diminished, though the effect of curvature on the later stages of transition and on turbulent transport downstream of transition is noticeable. Experiments were conducted with a zero streamwise pressure gradient, a constant-K ($K=\nu/U_\infty^2\, dU_\infty/dx$) of 0.75×10^{-6} and with a constant dU_∞/dx of 31 sec^{-1}. Various signal processing techniques were applied to both the hydrodynamic and heat transfer data. Probability density functions (PDF's) for temperature or velocity in the early transitional flow show a skewness, indicating the importance of a few, infrequent events for which the instantaneous velocity is low. In contrast, PDF's in fully-turbulent flow display a more Gaussian distribution, indicating a more uniform distribution with event size. Another processing technique is octant separation of turbulent shear stress and heat flux. In the transitional flow, an octant which represents a hot, wallward interaction, which is a rather unimportant octant in turbulent flow, emerges in importance. The importance of the hot wallward interaction remains when the flow is accelerated. Data on the combined effects of streamwise acceleration, concave curvature, and elevated free-stream disturbance levels were discussed. Profiles of the u'v' correlation show the separate effects of curvature and acceleration. A profile of u'v' processed from data taken from portions of the waveform for which u' is identified to be non-turbulent-like shows a small contribution of non-turbulent flow to the overall correlation value. Mean

temperature profiles show that if the acceleration effects on eddy diffusivity and the streamwise convection terms are included and if the turbulent Prandtl number measured by a triple-wire probe is employed, reasonable fits between the computed and measured profiles are attained. Power spectral distributions on u' are presented in fu'^2 v.s. log f coordinates (f is the frequency) and a peak in energy seems to roughly correspond to the frequency associated with convection of eddies of the integral scale size in the freestream. In an attempt to see the effect that the freestream may have on the boundary layer under such high bypass conditions, a ratio of the boundary layer spectrum to the freestream spectrum was taken. It appears to show considerable amplification at a frequency which roughly corresponds with that of the convected eddies. Further processing steps included computing the ratio of downstream to upstream spectra in the boundary layer divided by the same quantity but taken from the freestream data. The numerator shows the streamwise amplification in the boundary layer, the denominator shows the streamwise amplification in the freestream. It is interesting to note that the ratio remains at a value of 3 across the spectrum.

Upcoming activity includes measurements in stronger acceleration cases where a considerable transition length is expected in spite of the high disturbance level of the flow entering the test region.

Curvature Effect on Stanton Number
Tu=0.6%, Unaccelerated Flow

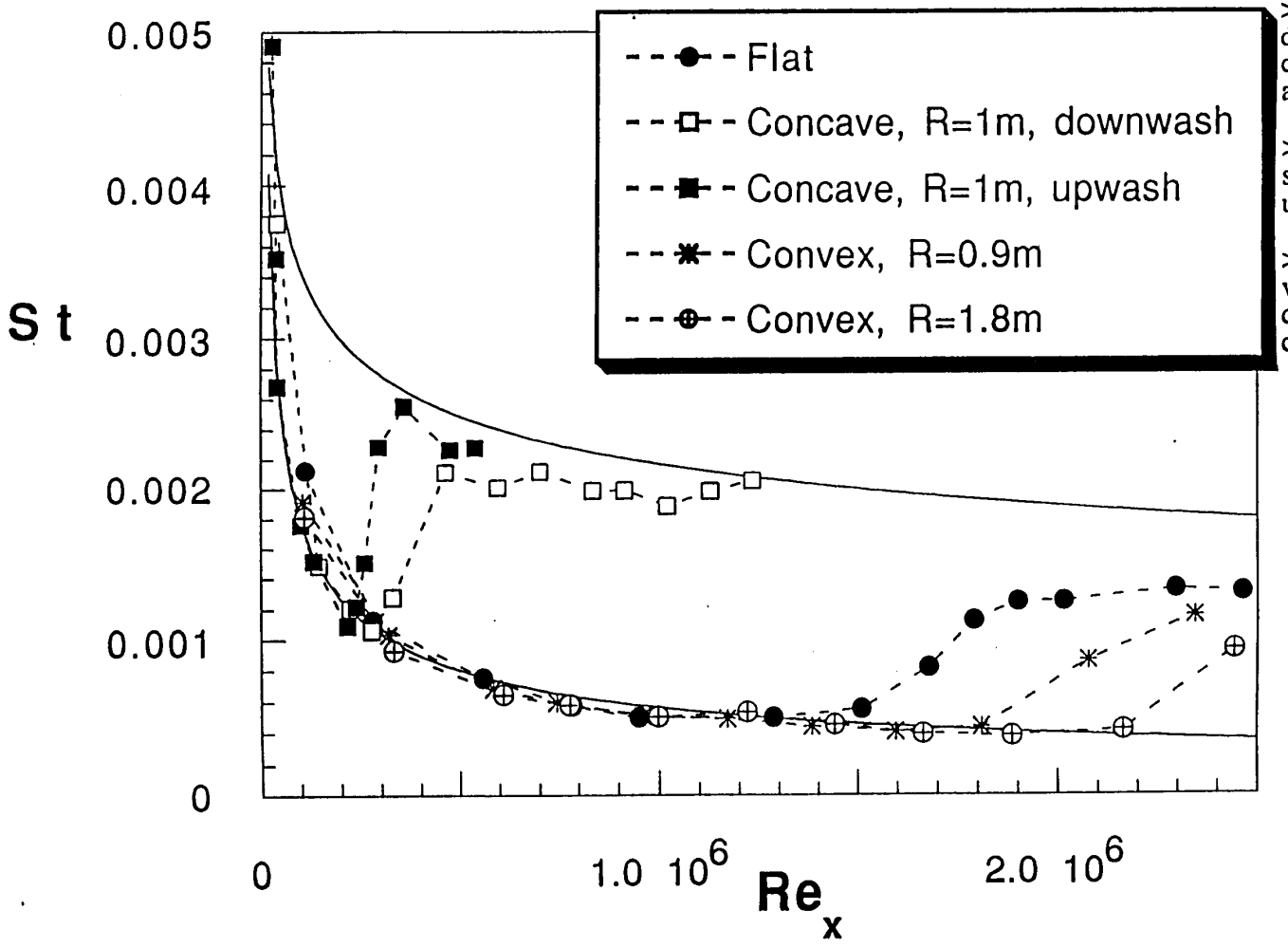

> Concave curvature is destabilizing, whereas convex curvature is stabilizing, relative to a flat wall.

> Concave case had an array of stationary Görtler vortices; hence, upwash and downwash regions.

> Convex effect should strengthen with magnitude of 1/R; hence, cases are out of order (R=0.9 m case is suspect).

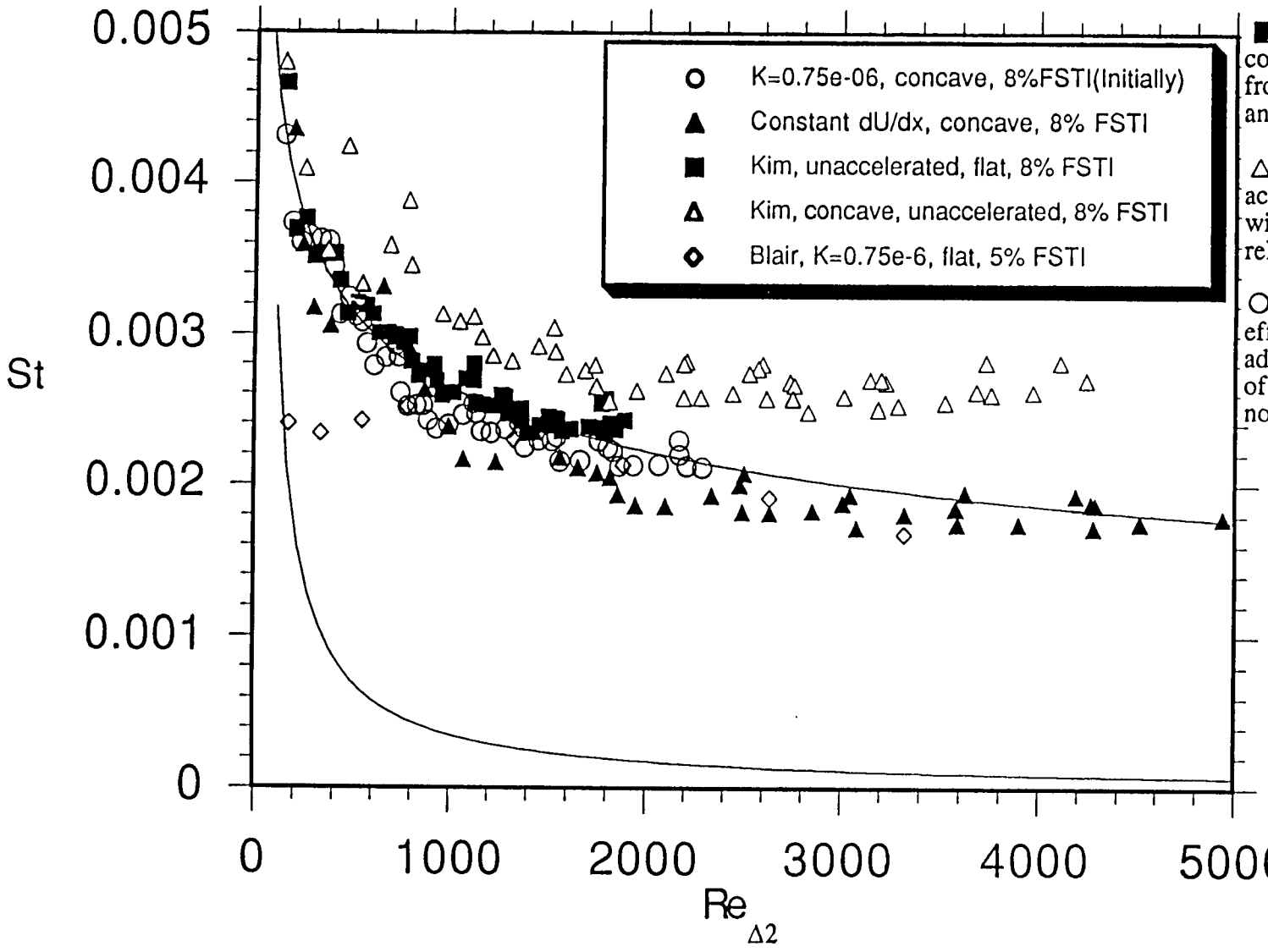

■ △ Comparison shows concave curvature effect (strong from very near the beginning -- and continually growing)

△ ▲○Comparison shows acceleration effect (decrease in St with increase of K, but no relaminarization tendencies)

○ ◇ Comparison shows an effect of slight FSTI rise and addition of curvature (note signs of transition in the ◇ case but no noticeable signs in the ○ case.

Stanton Numbers

OCTANT ANALYSIS

Instantaneous velocity and temperature signals divided into eight categories based on the signs of u', v' and t'.

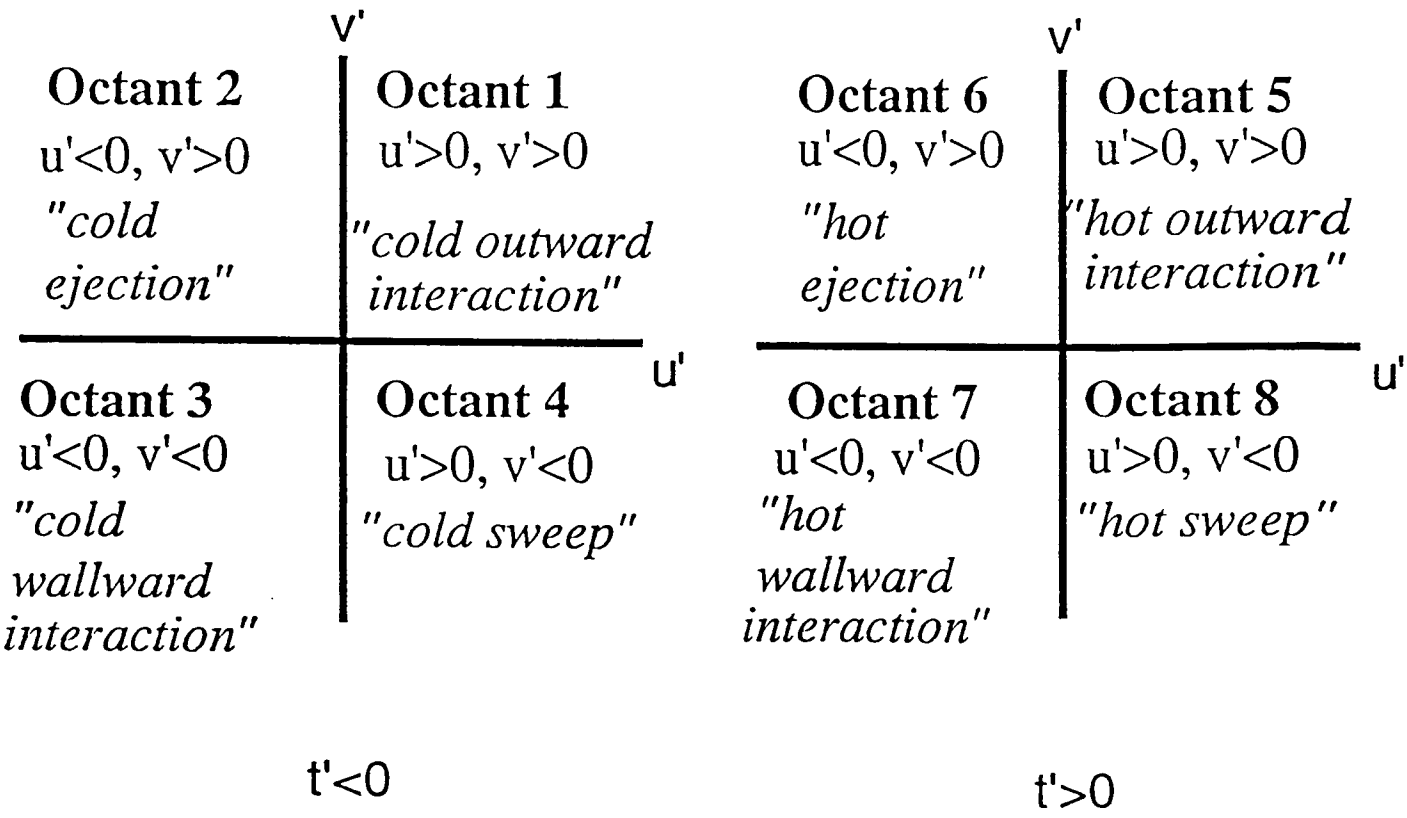

Names taken from Kawaguchi, Matsumori and Suzuki (1984).

Can correlate with particular eddy motions.

Examples of Ties to Flow Structure

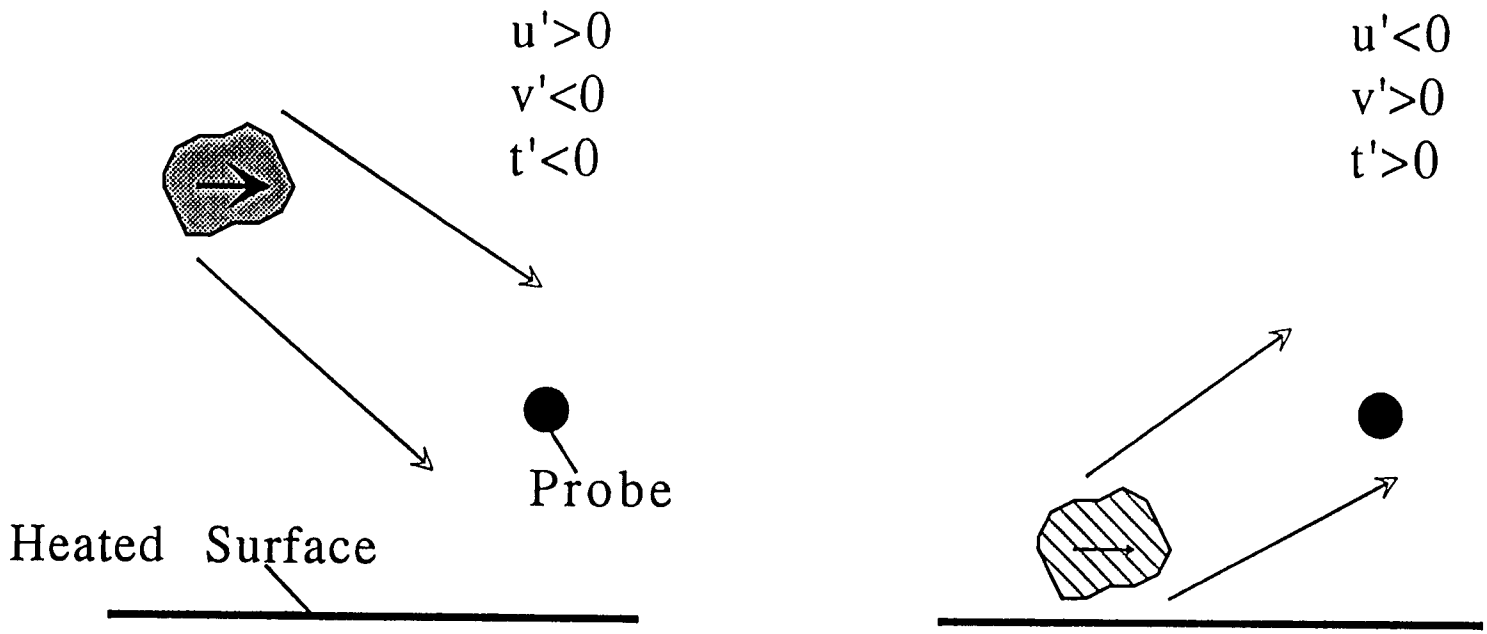

Octant 4
Cold Sweep

Octant 6
Hot Ejection

> These are the predominant terms in a turbulent boundary layer.

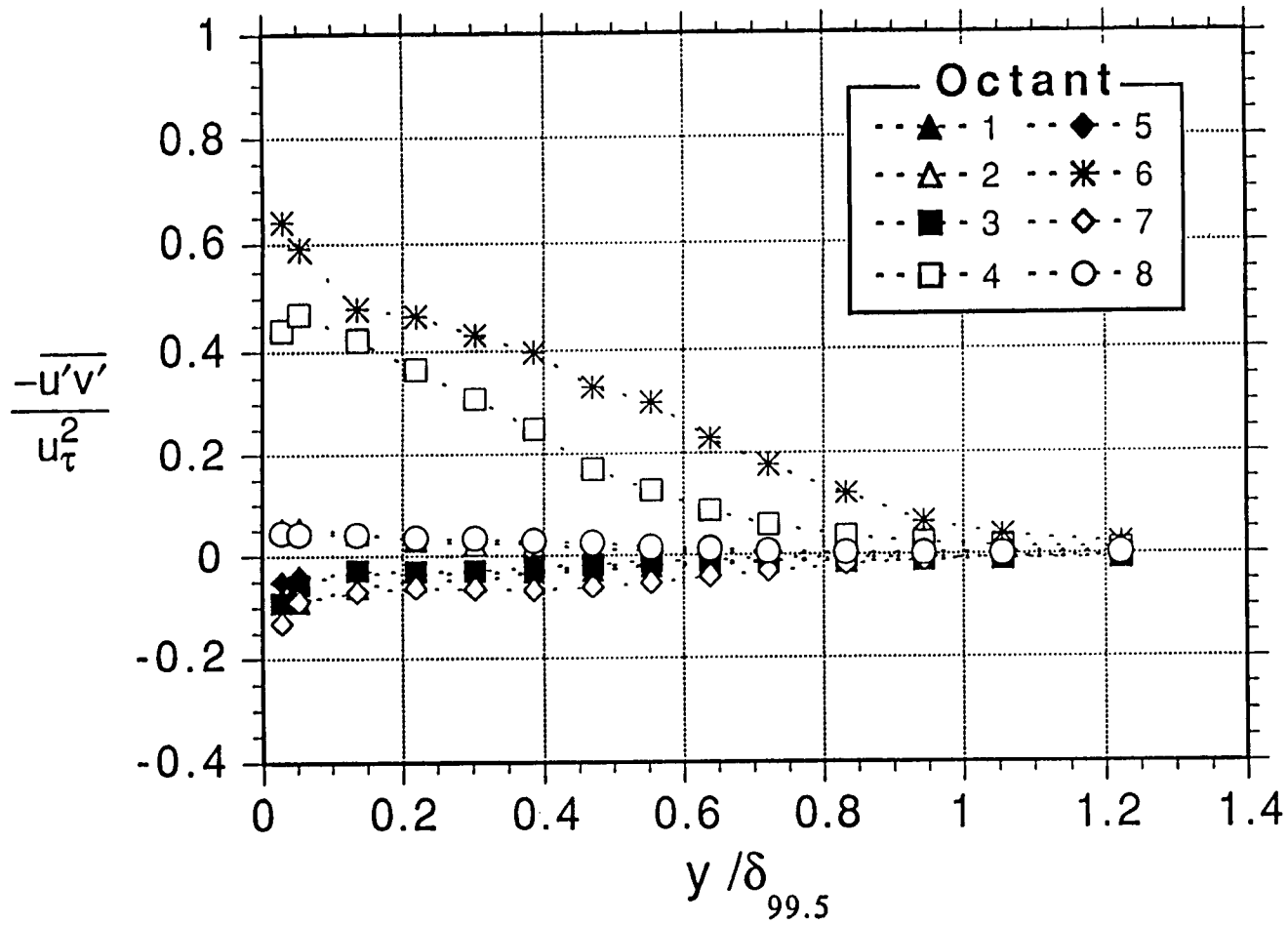

Turbulent shear stress profiles, 1.5% FSTI flat-wall case, fully-turbulent flow

Re_θ=1587, Re_x=1.062×10^6

> Note the importance of octants 4 and 6.

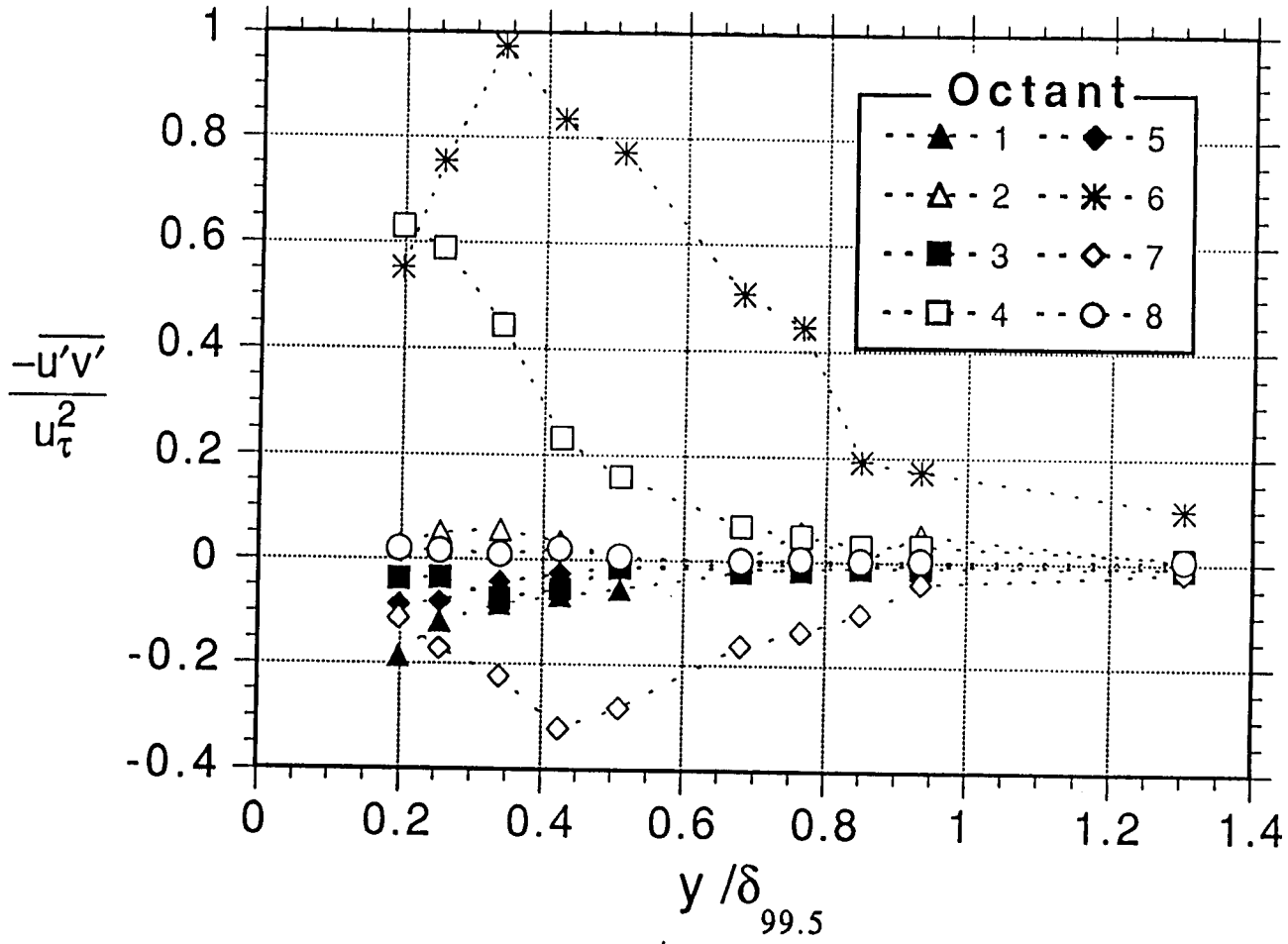

Turbulent shear stress profiles, 1.5% FSTI flat-wall case, transitional flow

Re_θ=379, Re_x=0.3442×10^6, γ=5% K=0.0

> Note the emergence of a positive $\overline{u'v'}$ contribution from octant 7 and the rise in importance of octant 6.

wo Wave Packet (TWP) Interaction; X=160cm Z=2cm Yma
Xp=30cm Zp=-4 and 8cm

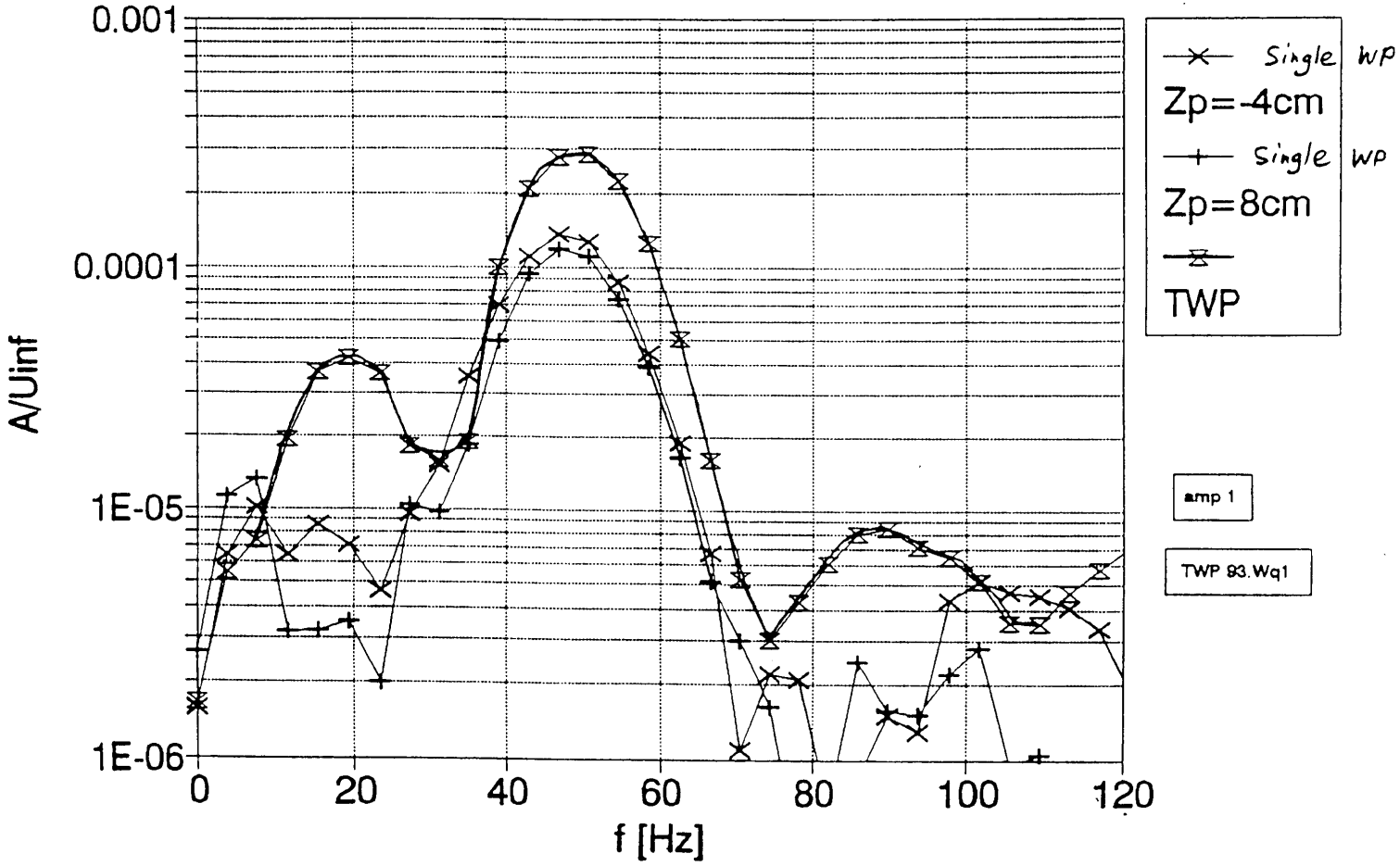

Appearance of a low band of f due to the Interaction

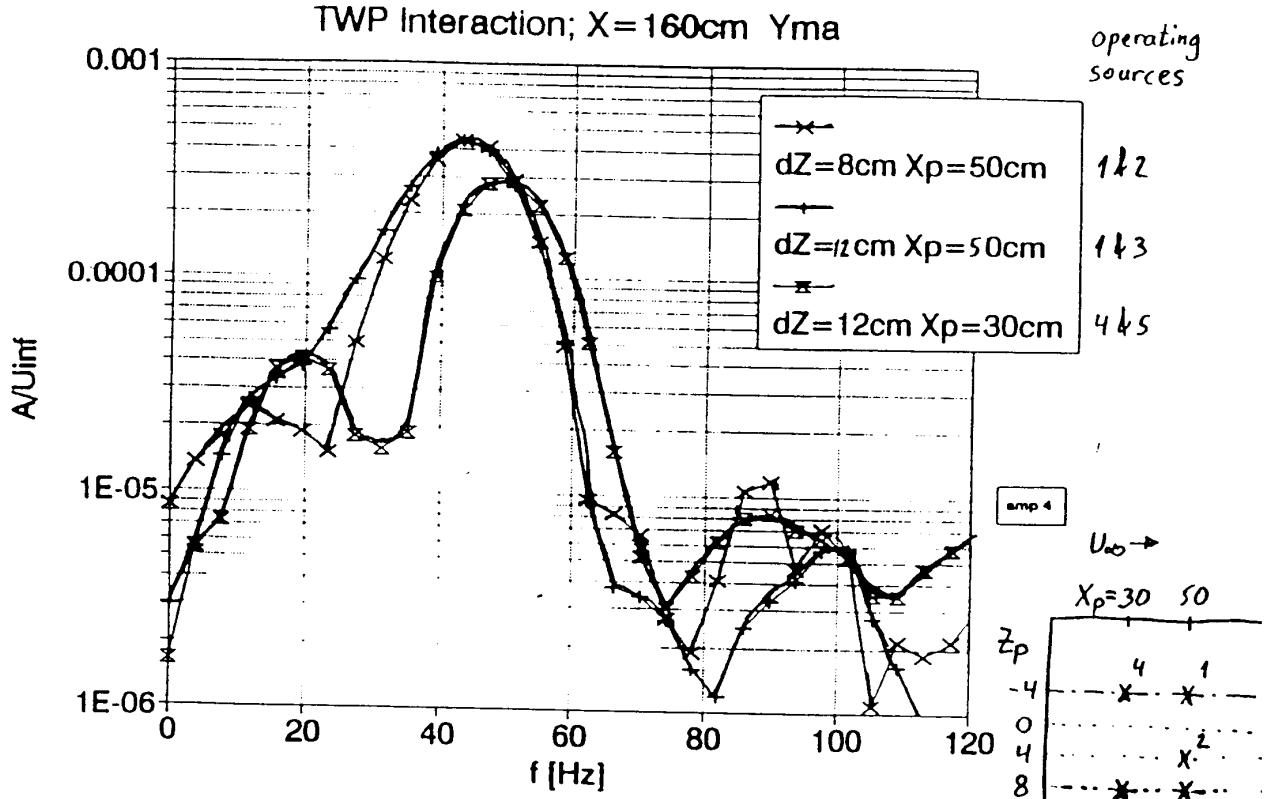

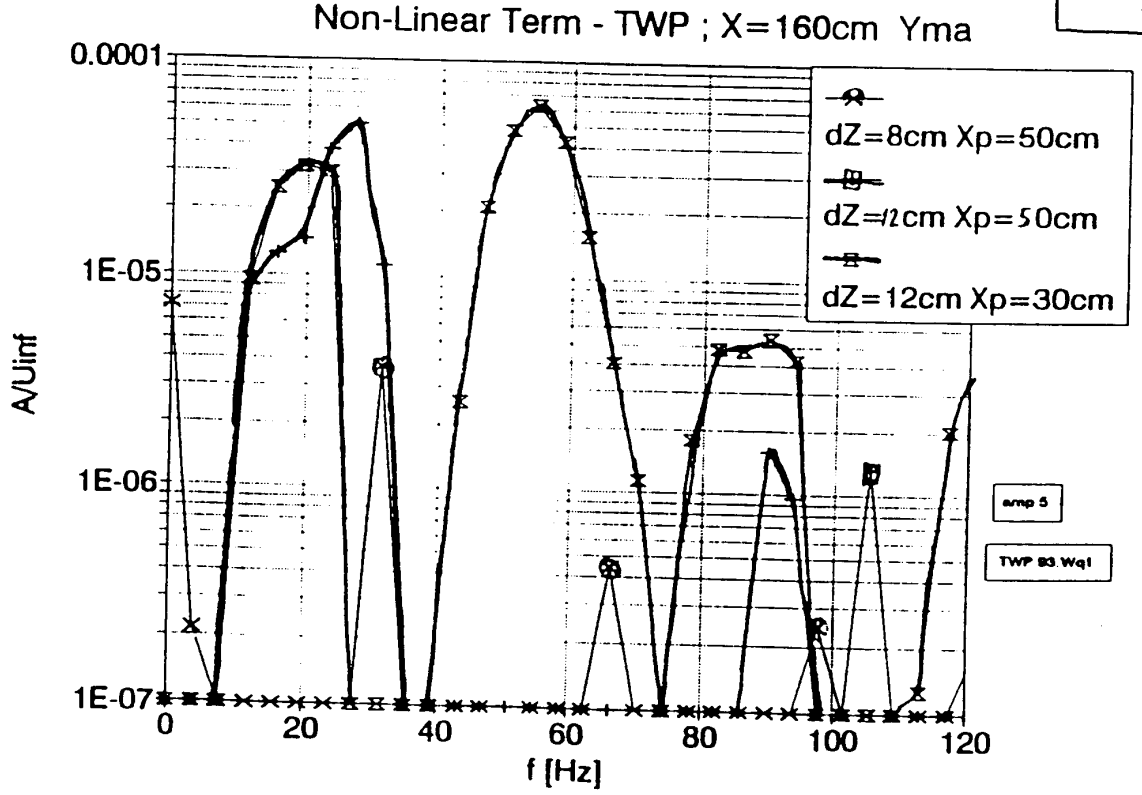

Effect of Spanwise Separation on Non-Linear term 12

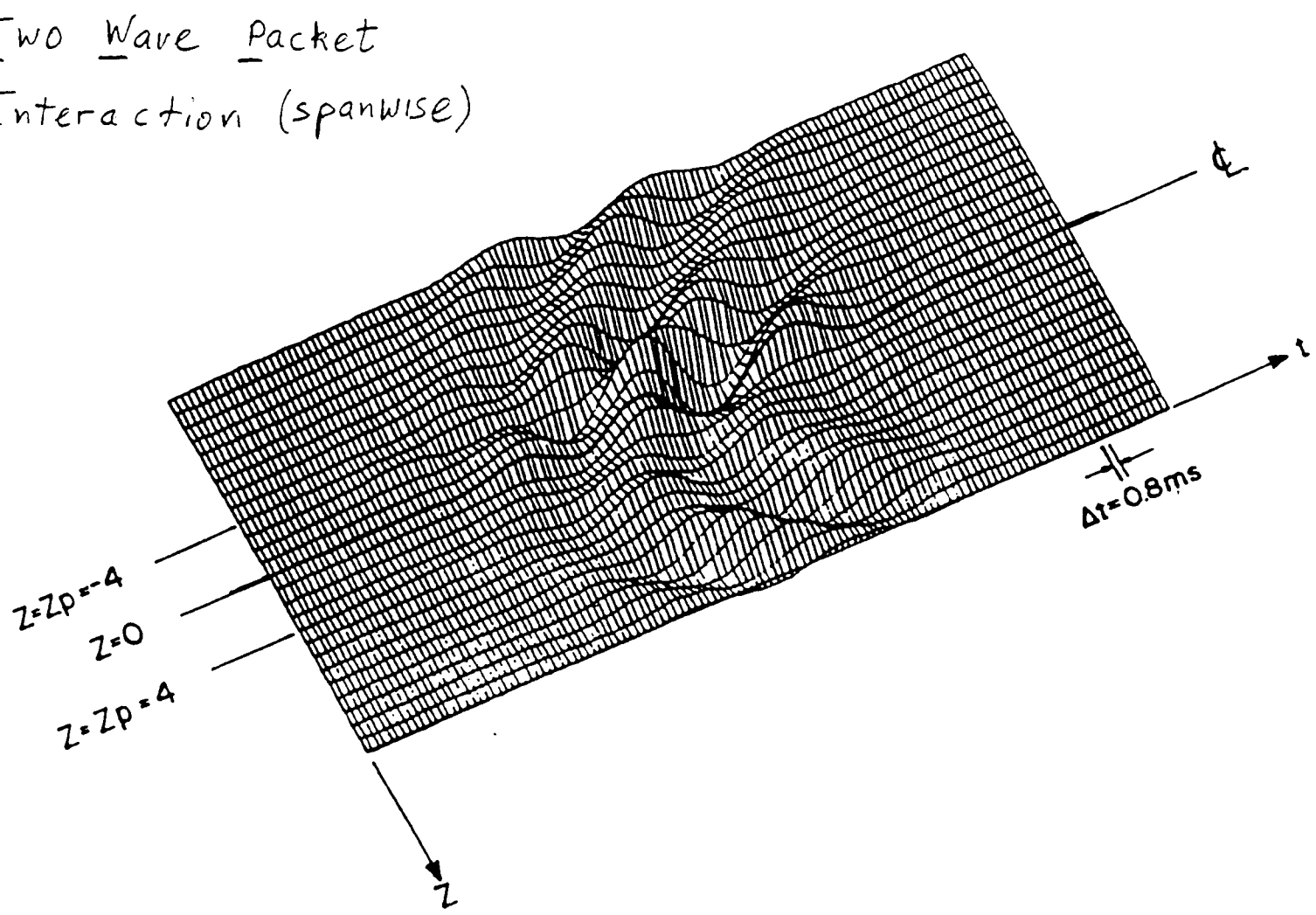

Fig. The velocity change due to the TWP passage at R_{δ^*}=1100 (X_s=55cm), Y≃Y_{max}, the whole TWP span. $U \sim 0.35 U_\infty$

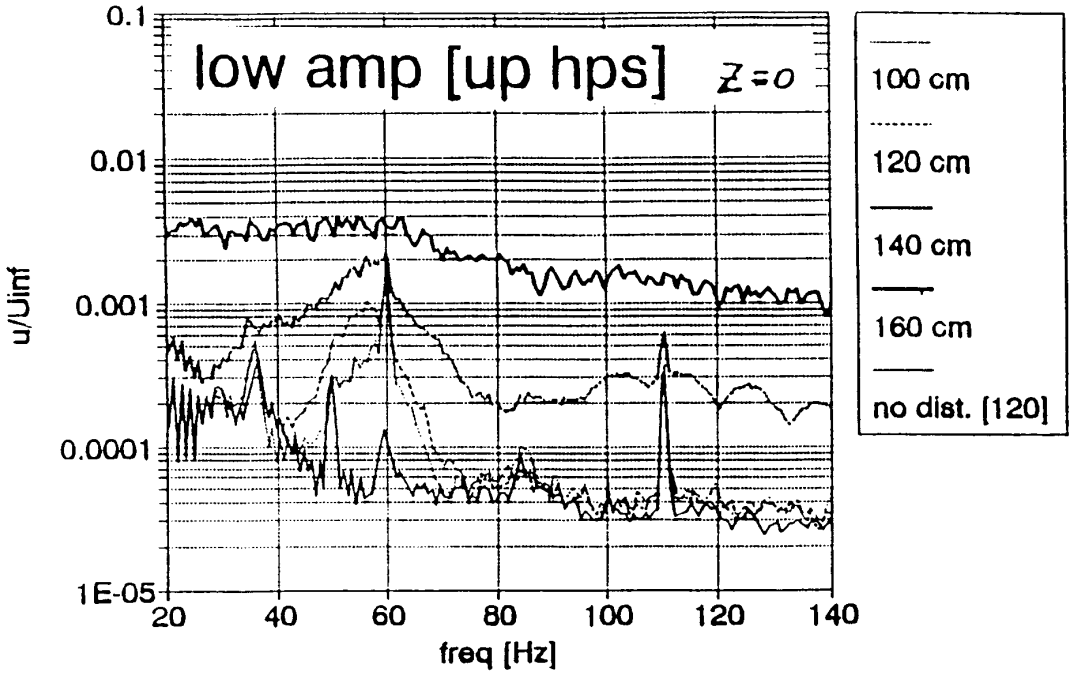

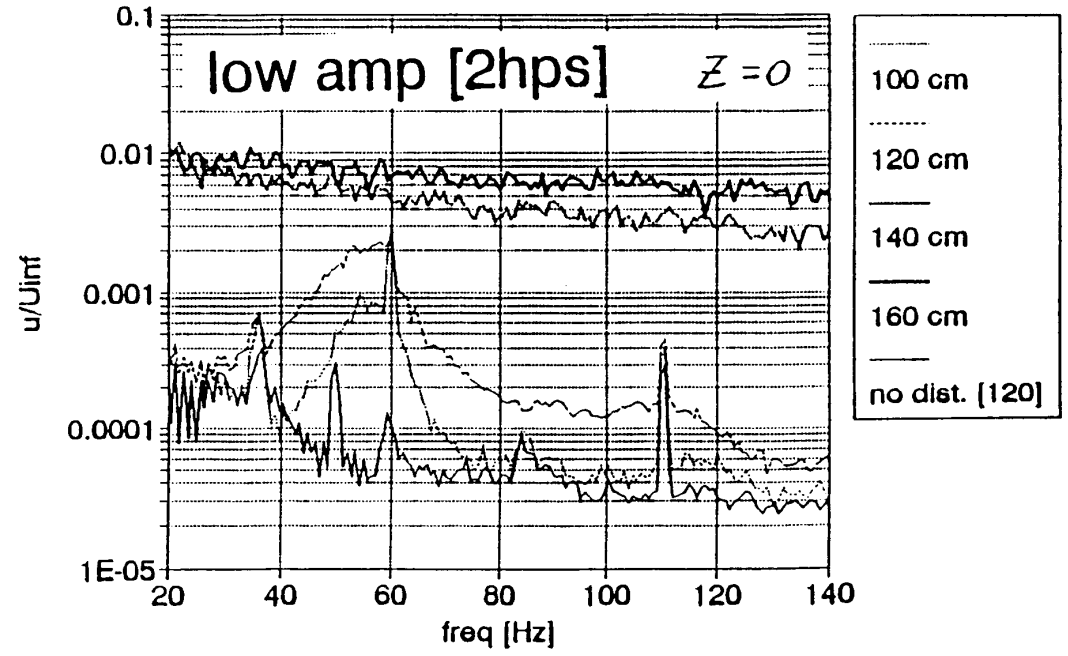

comparison between single HPS spectrum (up) and THPS (Interaction) spectrum.

9

PHASE LOCKED

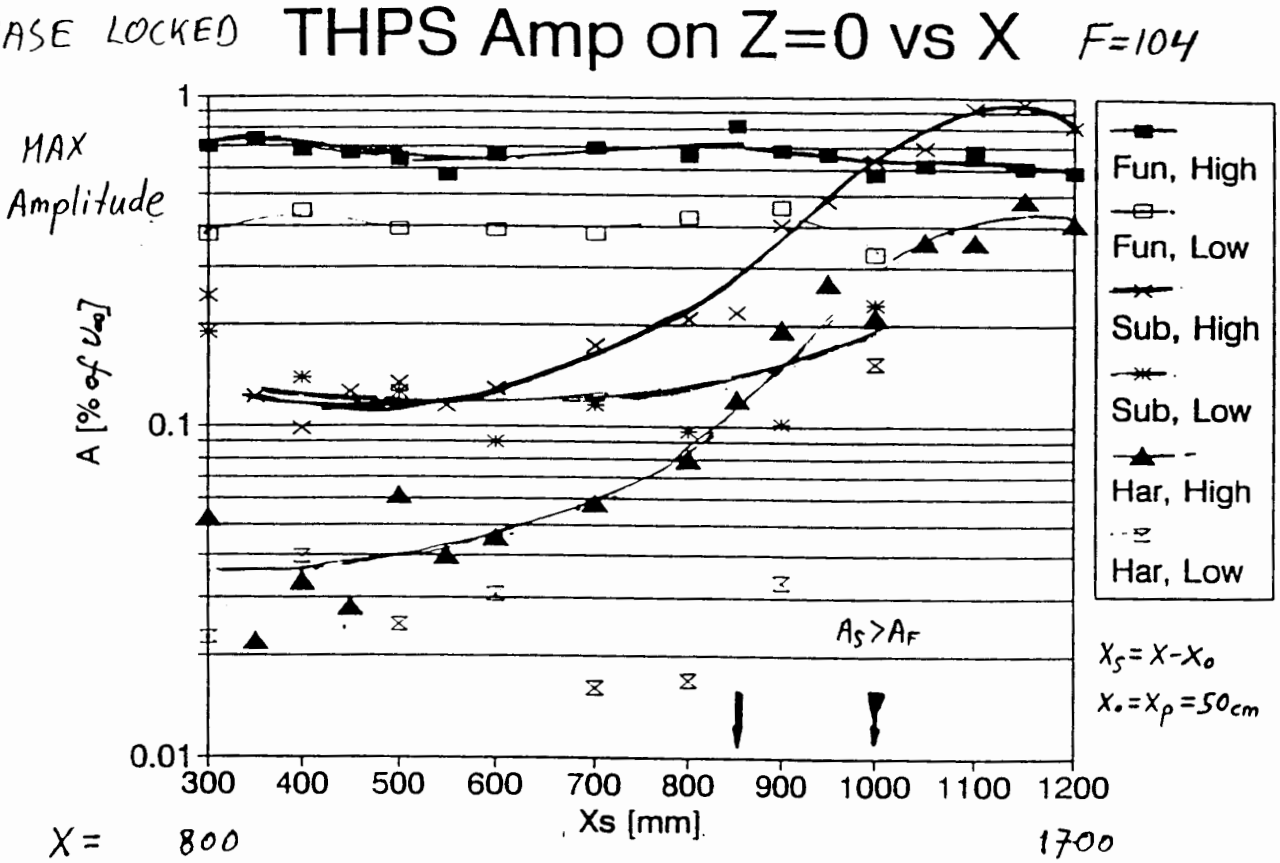

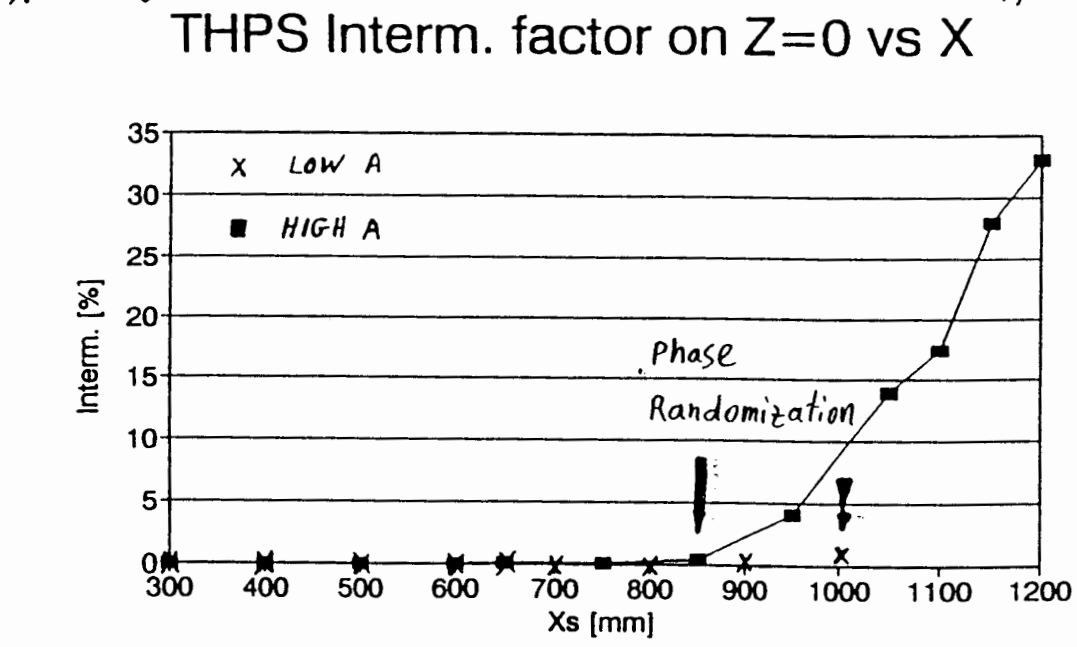

Two: Harmonic Point Source Interaction

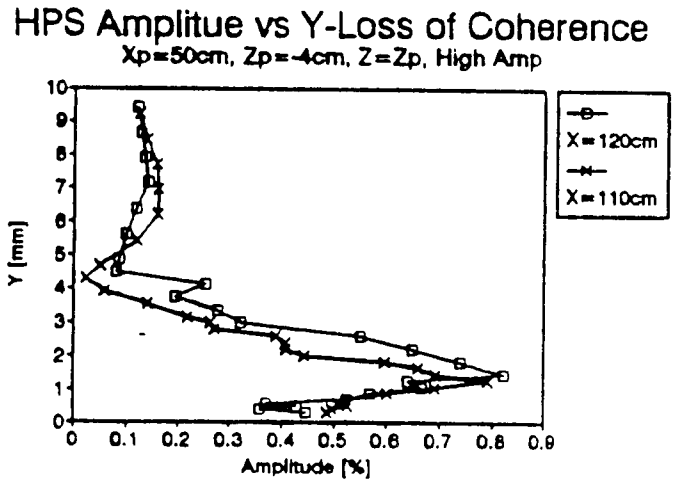

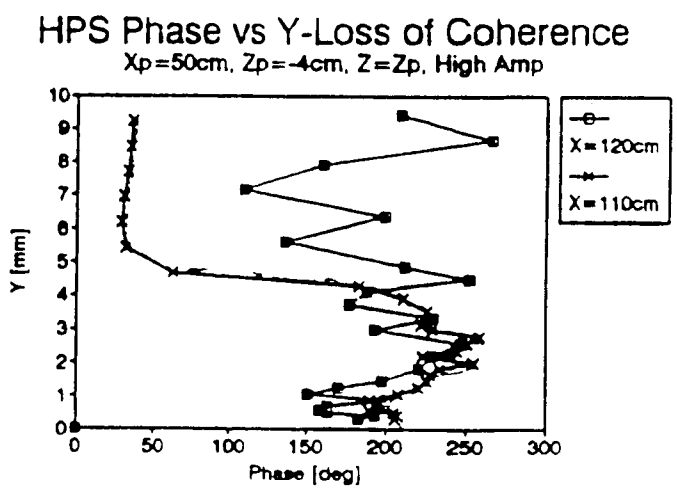

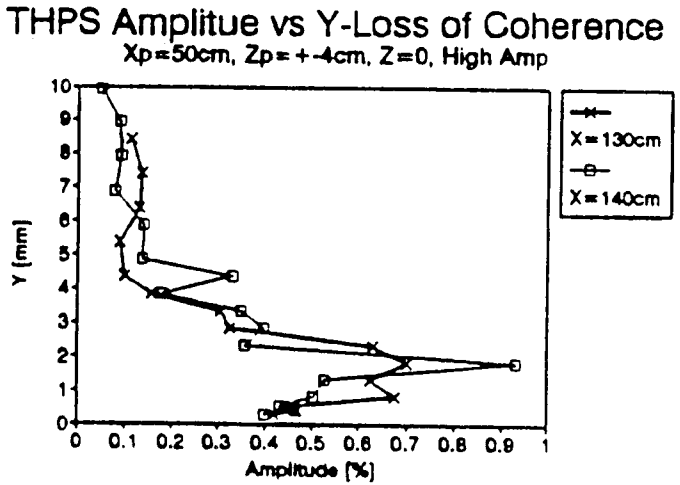

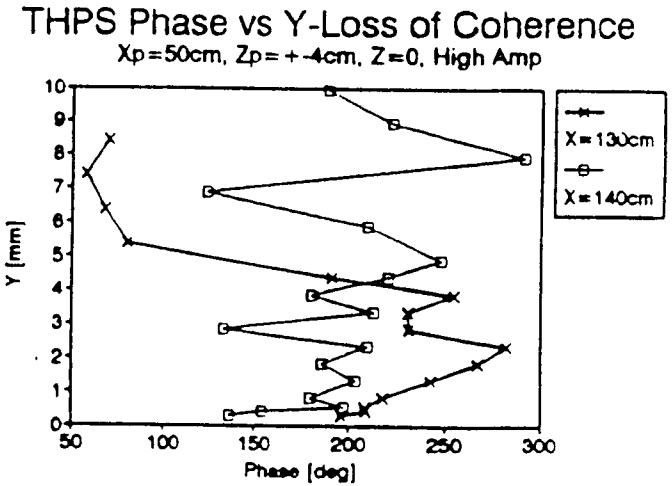

Phase Randomization prior to Breakdown

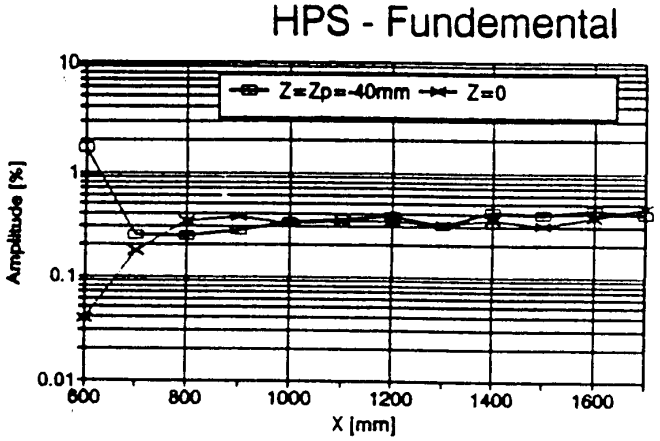

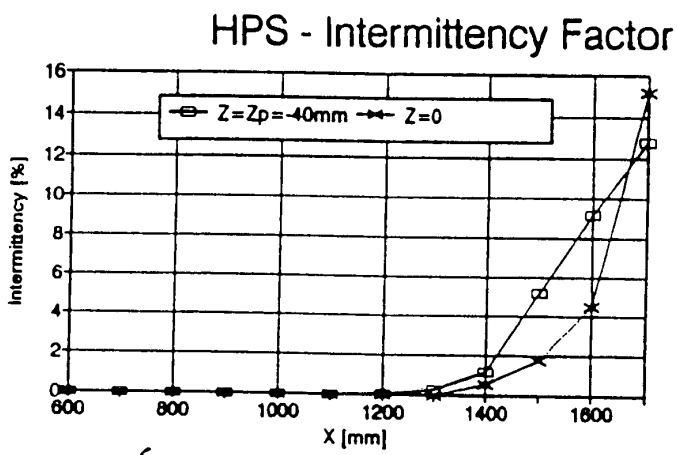

$F = 2\pi f \nu / U_\infty^2 = 104 \cdot 10^{-6}$

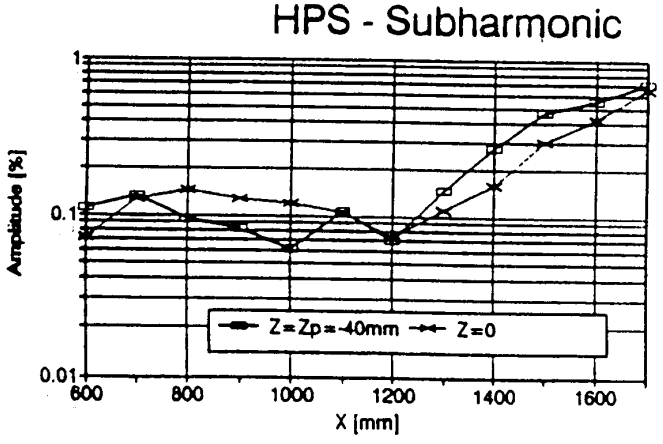

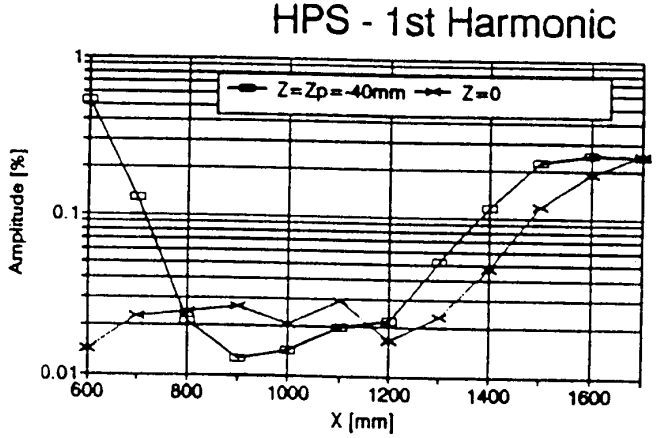

Max Amp (with respect to Y) Phase locked to the FUNDAMENTAL (F)

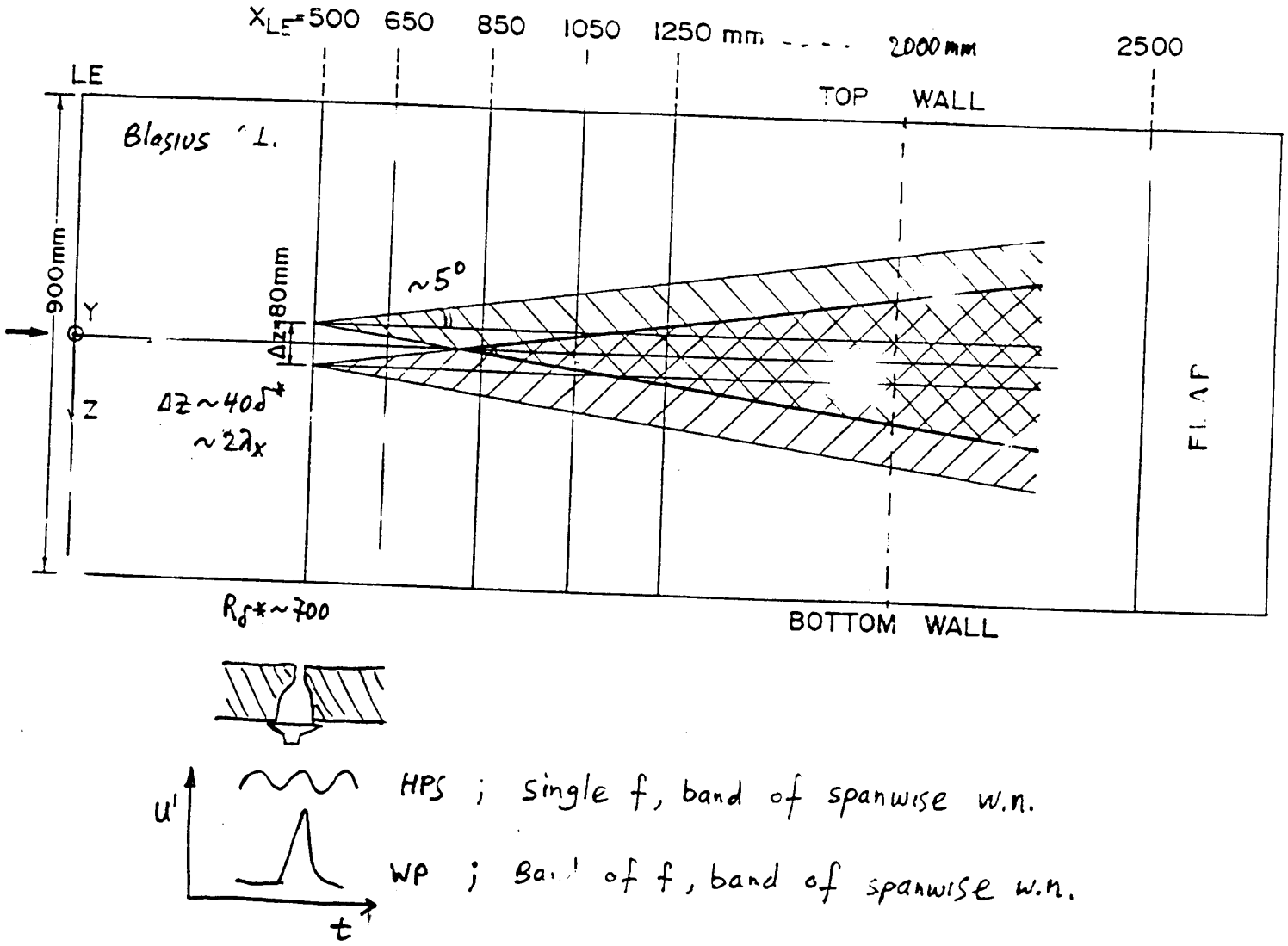
X_{LE}=500 650 850 1050 1250 mm ---- 2000 mm 2500
LE
TOP WALL
Blasius B.L.
900mm
Y
Z
J_∞
Δz 80mm
~5°
$\Delta z \sim 40\delta^*$
$\sim 2\lambda_x$
$R_{\delta^*} \sim 700$
BOTTOM WALL
FLAP
u'
t
HPS ; single f, band of spanwise w.n.
WP ; Band of f, band of spanwise w.n.